

NACA TN 3608 968E

TECH LIBRARY KAFB, NM  
0066447

# NATIONAL ADVISORY COMMITTEE FOR AERONAUTICS

TECHNICAL NOTE 3608

HYDRODYNAMIC IMPACT LOADS IN SMOOTH WATER FOR A PRISMATIC  
FLOAT HAVING AN ANGLE OF DEAD RISE OF  $10^\circ$

By Philip M. Edge, Jr.

Langley Aeronautical Laboratory  
Langley Field, Va.



Washington  
January 1956

AFMTC

TECHNICAL NOTE



## TECHNICAL NOTE 3608

HYDRODYNAMIC IMPACT LOADS IN SMOOTH WATER FOR A PRISMATIC  
FLOAT HAVING AN ANGLE OF DEAD RISE OF  $10^\circ$ 

By Philip M. Edge, Jr.

## SUMMARY

A prismatic float with an angle of dead rise of  $10^\circ$  was subjected to smooth-water impacts in the Langley impact basin. The investigation consisted of a series of impacts at fixed angles of trim of  $3^\circ$ ,  $12^\circ$ ,  $20^\circ$ , and  $30^\circ$  and at flight-path angles from  $2^\circ$  to  $23^\circ$ .

The data are tabulated and the variations of dimensionless coefficients with flight-path angle are compared with the theoretical variation. The experimental data are used to evaluate theoretical and empirical means of determining dead-rise function, aspect-ratio factor, and draft where chine-immersion effects will occur. Experimental values of dead-rise function and aspect-ratio factor are found to be in agreement with

$\frac{\pi}{2\beta} - 1$ , where  $\beta$  is angle of dead rise, and with Pabst's aspect-ratio

factor. In the determination of draft where chine-immersion effects will occur, an empirical value of dead-rise function for water pileup at an angle of dead rise of  $10^\circ$  and an angle of trim of  $3^\circ$  is obtained.

## INTRODUCTION

Theory indicates a sharp increase in the hydrodynamic load as the dead-rise angle approaches zero; however, there have been few experimental data available for verifying the loads predicted by theory for angles of dead rise below  $20^\circ$ . In order to obtain some data in the low dead-rise-angle range, a brief investigation of the loads in smooth water for an angle of dead rise of  $10^\circ$  was undertaken at the Langley impact basin. These data are compared with the theory for non-chine-immersed hydrodynamic impact presented in reference 1.

The determination of the actual loads and motions by application of theory involves the use of dead-rise function and aspect-ratio factors. Evaluations of these factors using experimental data for dead-rise angles of  $22\frac{1}{2}^\circ$ ,  $30^\circ$ , and  $40^\circ$  were presented in references 2, 3,

and 4, respectively. These evaluations indicate that existing theoretical dead-rise function and aspect-ratio factors, which are partly empirical, are satisfactory for predicting loads for these dead-rise angles. This paper presents experimental data obtained at a dead-rise angle of  $10^\circ$  and a comparison with theory. Included in this paper is an evaluation of the functions of dead rise and aspect-ratio factor in determining hydrodynamic load by non-chine-immersed theory. Comparisons with the chine-immersed branch curves of reference 1 are made and an empirical value of dead-rise function is computed for accounting for water pileup in predicting loads where chines are immersed.

#### SYMBOLS

A	hydrodynamic aspect ratio, $\frac{\tan \beta}{\tan \tau}$
c	wetted semiwidth of cross section
g	acceleration due to gravity, 32.2 ft/sec <sup>2</sup>
$n_i$	impact acceleration normal to water surface, g units
t	time after contact, sec
W	dropping weight, lb
$\dot{x}$	velocity of model parallel to water surface, fps
z	draft of model normal to water surface, ft
$\dot{z}$	velocity of model normal to water surface, fps
$\beta$	angle of dead rise, deg
$\gamma$	flight-path angle relative to water surface, deg
$\rho$	mass density of water, 1.938 slugs/cu ft
$\tau$	trim angle, deg
$f(\beta)$	dead-rise function for determining loads
$h(\beta)$	dead-rise function for determining water rise
$\phi(A)$	aspect-ratio factor

## Subscripts:

ch conditions at instant of chine immersion

o at water contact

s conditions at step

max maximum

## Dimensionless variables:

Approach parameter

$$\kappa = \frac{\sin \tau}{\sin \gamma_0} \cos (\tau + \gamma_0)$$

Load-factor coefficient

$$C_l = \frac{n_1 g}{z_0^2} \left( \frac{W}{g} \left\{ \frac{6 \sin \tau \cos^2 \tau}{[\bar{f}(\beta)]^2 \varphi(A) \rho \pi} \right\} \right)^{1/3}$$

Draft coefficient

$$C_d = z \left( \frac{g}{W} \left\{ \frac{[\bar{f}(\beta)]^2 \varphi(A) \rho \pi}{6 \sin \tau \cos^2 \tau} \right\} \right)^{1/3}$$

Draft coefficient at chine immersion

$$C_{d, ch} = c_{s, ch} \left\{ \frac{g}{W} \left[ \frac{\varphi(A) \rho \pi}{6 h(\beta) \tan \tau} \right] \right\}^{1/3}$$

Time coefficient

$$C_t = t z_0 \left( \frac{g}{W} \left\{ \frac{[\bar{f}(\beta)]^2 \varphi(A) \rho \pi}{6 \sin \tau \cos^2 \tau} \right\} \right)^{1/3}$$

## APPARATUS

The data were obtained from a series of runs in the Langley impact basin which is described in reference 5.

The model tested was a prismatic float having a dead-rise angle of  $10^\circ$ , a beam of 3.4 feet, and a weight of 1,205 pounds. The lines of the model are shown in figure 1.

The instrumentation used to determine horizontal and vertical displacements and velocities was described in reference 5. Accelerations in the vertical direction were measured by an electrical accelerometer of the unbonded strain-gage type having a natural frequency of approximately 85 cycles per second. The contact and exit of the model were determined by means of an electrical circuit completed by the water. A multichannel oscillograph having 0.01-second timing was used to record the measurements of each of the instruments.

### PRECISION

The instrumentation used in the investigation gives measurements that are believed to be accurate within the following limits:

Horizontal velocity, fps . . . . .	$\pm 0.5$
Vertical velocity, fps . . . . .	$\pm 0.2$
Weight, lb . . . . .	$\pm 2.0$
Acceleration, g units . . . . .	$\pm 0.3$
Time, sec . . . . .	$\pm 0.005$
Vertical displacement, ft . . . . .	$\pm 0.02$

### TEST PROCEDURE

The investigation consisted of a series of impacts in smooth water at fixed angles of trim of  $3^\circ$ ,  $12^\circ$ , and  $30^\circ$ . The flight-path angle was varied from  $2^\circ$  to  $23^\circ$  with forward speeds ranging from 25 feet per second to 97 feet per second.

The model was attached to the carriage by a parallel linkage restraining the model in all directions except vertical. The carriage was catapulted up to testing speed where the parallel-linkage action permitted the model to fall freely in the vertical direction until the desired vertical velocity was acquired. At this point in the descent of the model, a vertical force of 1 g was applied by a compressed-air lift engine. In this manner, impacts were made under conditions simulating landings in which the wing lift is equal to the weight of the airplane. This testing procedure is described in more detail in reference 5.

## RESULTS AND COMPARISONS WITH THEORY

The basic data obtained in this investigation are presented in table I. Included in this table are the initial horizontal velocity and vertical velocity, the vertical acceleration and drafts at instants of maximum acceleration and maximum draft, and the times to maximum acceleration, to maximum draft, and to rebound. It should be remembered that an angle of dead rise of  $10^\circ$  is small, and at low angles of dead rise the hydrodynamic load becomes very sensitive to the dead-rise function and the aspect-ratio factor. Although the model and testing range (beam loading, flight-path angles, and trim angle) of this investigation were similar to those of previous investigations (refs. 1 to 4), the likelihood of chine immersion is much greater because of the low angle of dead rise. With these points in mind, the data are presented as dimensionless coefficients and are compared with non-chine-immersed theory in the form of plots against the approach parameter  $\kappa$ . The approach parameter was introduced in reference 1 as a single parameter governing the dimensionless variables of motion and time. The approach parameter, a function of the trim and initial flight-path angle, is used to obtain a single curve for each of the variations of dimensionless displacements, velocities, and accelerations, regardless of seaplane properties, attitude, or initial velocity.

The variation of the load-factor coefficient with approach parameter is presented in figure 2. The trend of the experimental points follows the theoretical variation of the maximum load-factor coefficient and the load-factor coefficient at the time of maximum draft. The data obtained at maximum acceleration are in good agreement with theory at high values of  $\kappa$ . However, at low values of  $\kappa$  (high flight-path angle), the data fall almost 20 percent below the non-chine-immersed curve and along the chine-immersed branch curves. Since the theory of reference 1 predicts no chine immersion for these conditions, disagreement with theory is indicated and these runs will be discussed subsequently. The data obtained at maximum draft are in good agreement with theory at high values of  $\kappa$ , but scatter about the theory at low values of  $\kappa$ .

The variation of the draft coefficient with approach parameter is shown in figure 3. The trend of the experimental data follows the trend of the theoretical variation. However, the fact that the experimental data fall above the theoretical curve indicates greater depths of penetration than those predicted by theory. Although increased depth of penetration at maximum draft can be expected because of chine immersion at the lower values of  $\kappa$ , the experimental data show greater drafts throughout the range at both maximum acceleration and maximum draft.

The variation of the time coefficient with approach parameter is shown in figure 4. The experimental data are presented for the instants

of maximum acceleration, maximum draft, and rebound from the water. The trend of the experimental data is in good agreement with the theoretical variation. The fact that the data at low values of  $\kappa$  (high flight-path angle) again fall away from the theoretical curve indicates later times at each of the instants. These increased times are in agreement with the increased draft shown in figure 3.

The ratio of vertical velocity to initial vertical velocity is shown in figure 5 plotted against the approach parameter. The upper curve shows the variation at the instant of maximum acceleration and the lower curve shows the variation at the instant of rebound. The experimental data are in reasonable agreement with the theoretical variation.

### ANALYSIS OF RESULTS

The prediction of hydrodynamic loads is dependent upon theoretical or empirical means of determining dead-rise function, aspect-ratio factor, and draft where chine-immersion effects will occur. The experimental data obtained in this investigation offer an opportunity to evaluate these theoretical quantities for conditions where few data have previously been available. In order to evaluate these quantities, the data are divided into three parts: First, non-chine-immersed data for an angle of trim of  $3^\circ$  where aspect-ratio factor is of little consequence are used to determine an experimental dead-rise function; second, the higher trim non-chine-immersed data where aspect-ratio factor is appreciable are used to obtain an experimental value of  $\phi(A)$ ; and third, the chine-immersed data are analyzed and an empirical value of dead-rise function is computed for the prediction of draft where chine immersion will occur.

#### Effect of Dead-Rise Function and Aspect-Ratio

##### Factor on Hydrodynamic Load

The relationship of hydrodynamic load to dead-rise function and aspect-ratio factor is shown by the following equation (see ref. 1):

$$C_L = \frac{n_1 g}{z_0^2} \left( \frac{W}{g} \left\{ \frac{6 \sin \tau \cos^2 \tau}{[f(\beta)]^2 \phi(A) \rho \pi} \right\} \right)^{1/3} \quad (1)$$

This equation shows that the hydrodynamic load  $n_1$  varies as the two-thirds power of the dead-rise function and as the one-third power of the aspect-ratio factor. With the use of theoretical quantities for

$f(\beta)$  and  $\varphi(A)$ , hydrodynamic loads can be predicted from this equation. In order to obtain an understanding of the theoretical quantities used for  $f(\beta)$  and  $\varphi(A)$ , consideration is given to their variation as the dead-rise angle is lowered to  $10^\circ$ .

The quantity widely used as function of dead rise is  $f(\beta) = \frac{\pi}{2\beta} - 1$  (ref. 6). The variation of  $\left(\frac{\pi}{2\beta} - 1\right)^{2/3}$  with angle of dead rise is shown in figure 6. The application of  $\left(\frac{\pi}{2\beta} - 1\right)^{2/3}$  in predicting loads has been experimentally verified for angles of dead rise of  $22\frac{1}{2}^\circ$  to  $40^\circ$  (refs. 1 to 4); however, below  $22\frac{1}{2}^\circ$ , figure 6 shows large increases in  $[f(\beta)]^{2/3}$  which in turn mean large increases in load as can be seen from equation (1). Since this curve approaches infinity as zero dead-rise or flat-plate condition is approached, it becomes unrealistic in the extremely low dead-rise range and a need for determining the lower limits for which this quantity can be applied to the determination of loads is evident. A purpose of this analysis is to obtain an experimental value of  $f(\beta)$  for an angle of dead rise of  $10^\circ$  and to compare this value with  $\frac{\pi}{2\beta} - 1$ .

An expression for aspect-ratio factor was obtained by Pabst in reference 7 and is given by the quantity

$$\varphi(A) = \left(\frac{1}{1 + \frac{1}{A^2}}\right)^{1/2} \left(1 - \frac{0.425}{A + \frac{1}{A}}\right) \quad (2)$$

An approximation of  $\varphi(A)$  was given by Pabst for the V-bottom float as

$$\varphi(A) = \left(1 - \frac{\tan \tau}{2 \tan \beta}\right) \quad (3)$$

where it is assumed that the end-flow correction is determined by the shape of the intersected area in the plane of the water surface. The variation of the load as influenced by these expressions as the angle of dead rise is lowered from  $40^\circ$  to  $10^\circ$  is shown in figure 7; the dashed curves show the V-bottom approximation pulling sharply away from the general expression at low dead-rise angles and high angles of trim. This figure shows that at an angle of dead rise of  $10^\circ$  the V-bottom approximation is very poor for trim angles above  $12^\circ$ . It is further observed from this figure that Pabst's expression for  $\varphi(A)$  indicates



that at a low angle of trim, such as  $3^\circ$ , the  $\varphi(A)$  factor for determining load is very close to unity even at an angle of dead rise of  $10^\circ$ . Therefore,  $\varphi(A)$  has little influence on hydrodynamic force on a model at an angle of trim of  $3^\circ$ , and small errors in the value of  $\varphi(A)$  used would have negligible effect on determination of loads. From these data, an experimental value of  $f(\beta)$  can be obtained from equation (1) by using the experimental value of  $n_1$  and a theoretical value of  $C_L$  corresponding to the approach parameter  $\kappa$ .

Experimental values of  $[f(\beta)]^{2/3}$  were obtained for the several non-chine-immersed runs at  $3^\circ$  of trim of this investigation and were found to agree with  $\left(\frac{\pi}{2\beta} - 1\right)^{2/3}$  within the accuracy of the experimental data. This agreement indicates that the function of dead-rise angle in determining the hydrodynamic load is closely represented by  $f(\beta) = \frac{\pi}{2\beta} - 1$  for an angle of dead rise of  $10^\circ$ .

After the data where  $\varphi(A)$  was of little consequence were used and verification of the dead-rise function  $\frac{\pi}{2\beta} - 1$  at an angle of dead rise of  $10^\circ$  was established, this value of the dead-rise function was substituted into equation (1) and experimental values of  $[\varphi(A)]^{1/3}$  were obtained for higher angles of trim where the  $\varphi(A)$  function has a large effect on the hydrodynamic load. In this manner, the data obtained from the runs in which the angles of trim were  $12^\circ$ ,  $20^\circ$ , and  $30^\circ$  where chines were not immersed were substituted into equation (1) and the resulting experimental values of  $[\varphi(A)]^{1/3}$  are presented in figure 8 where a comparison is made with Pabst's empirical expression. This figure shows substantial agreement between the experimental values of  $\varphi(A)$  obtained from this investigation and those obtained from the empirical expression derived by Pabst.

#### Chine Immersion

The runs made in this investigation were runs where the theory of reference 1 predicted no effect of chine immersion on load; however, the data above a flight-path angle of  $5^\circ$  indicated an effect of chine immersion on load. The possibility of chine-immersion effect on maximum load was determined theoretically by solving for the draft coefficient at the instant of chine immersion (see ref. 1):

$$C_{d, ch} = c_{s, ch} \left\{ \frac{g}{W} \left[ \frac{\varphi(A) \rho \pi}{6 f(\beta) \tan \tau} \right] \right\}^{1/3} \quad (4)$$

If  $C_{d, ch}$  is greater than the draft coefficient at which the maximum load-factor coefficient occurs ( $C_{d, ch} \geq 0.65$ ), there will be no effect of chine immersion on maximum load. The effect of chine immersion on maximum load-factor coefficient is shown by the theoretical curves of reference 1 presented in figure 2. The experimental data for an angle of trim of  $3^\circ$  are shown to lie below the non-chine-immersed curve. Although  $C_{d, ch}$  is greater than 0.65 for an angle of dead rise of  $10^\circ$  and an angle of trim of  $3^\circ$ , the experimental data show a reduction in maximum load-factor coefficient corresponding to a value of  $C_{d, ch}$  of approximately 0.475. This occurrence of chine immersion indicates that  $f(\beta) = \frac{\pi}{2\beta} - 1$  is not sufficiently large to account for water pileup for an angle of dead rise of  $10^\circ$  at an angle of trim of  $3^\circ$ . Since  $f(\beta) = \frac{\pi}{2\beta} - 1$  does not account for water pileup, equation (4) can be rewritten as

$$C_{d, ch} = c_{s, ch} \left\{ \frac{g}{W} \left[ \frac{\varphi(A) \rho \pi}{6 h(\beta) \tan \tau} \right] \right\}^{1/3} \quad (5)$$

where  $h(\beta)$  is the dead-rise correction for water pileup for the condition with an angle of dead rise of  $10^\circ$  and an angle of trim of  $3^\circ$ .

Solving equation (5) for  $[h(\beta)]^{1/3}$  gives

$$[h(\beta)]^{1/3} = \frac{c_{s, ch}}{C_{d, ch}} \left\{ \frac{g}{W} \left[ \frac{\varphi(A) \rho \pi}{6 \tan \tau} \right] \right\}^{1/3} \quad (6)$$

and a value of  $[h(\beta)]^{1/3} = 2.74$  is obtained as the empirical value corresponding to the  $C_{d, ch}$  value of 0.475 from the experimental data.

This value indicates a 37-percent increase in the dead-rise correction for water pileup as compared with that predicted by  $[f(\beta)]^{1/3}$  for an angle of dead rise of  $10^\circ$  at an angle of trim of  $3^\circ$ . Since  $h(\beta)$  is 2.5 times  $f(\beta)$ , equation (5) can be written

$$C_{d, ch} = c_{s, ch} \left\{ \frac{g}{W} \left[ \frac{\varphi(A) \rho \pi}{15 f(\beta) \tan \tau} \right] \right\}^{1/3}$$

for an angle of dead rise of  $10^\circ$  and an angle of trim of  $3^\circ$ .

The experimental data obtained at angles of trim of  $12^\circ$ ,  $20^\circ$ , and  $30^\circ$  consisted of too few runs for water-pileup or chine-immersion analysis.

### CONCLUSIONS

An analysis of experimental data obtained from an investigation of hydrodynamic impact loads in smooth water for a float having an angle of dead rise of  $10^\circ$  results in the following conclusions:

1. The expression  $\frac{\pi}{2\beta} - 1$  appears to be a fair approximation of the function of dead-rise angle  $f(\beta)$  in the determination of hydrodynamic load.
2. Experimental values of an aspect-ratio factor  $\varphi(A)$  show substantial agreement with the empirical expression derived by Pabst.
3. In the determination of draft where chine-immersion effects will occur, an empirical value of  $h(\beta) = 2.5 f(\beta)$  is obtained as a function of dead-rise angle for water pileup at an angle of trim of  $3^\circ$ .
4. The trend of the experimental variation of load-factor coefficient, draft coefficient, time coefficient, and velocity ratio are in good agreement with the theoretical variation.

Langley Aeronautical Laboratory,  
National Advisory Committee for Aeronautics,  
Langley Field, Va., October 11, 1955.

## REFERENCES

1. Milwitzky, Benjamin: A Generalized Theoretical and Experimental Investigation of the Motions and Hydrodynamic Loads Experienced by V-Bottom Seaplanes During Step-Landing Impacts. NACA TN 1516, 1948.
2. Mayo, Wilbur L.: Theoretical and Experimental Dynamic Loads for a Prismatic Float Having an Angle of Dead Rise of  $22\frac{1}{2}^{\circ}$ . NACA WR L-70, 1945. (Formerly NACA RB L5F15.)
3. Miller, Robert W., and Leshnover, Samuel: Hydrodynamic Impact Loads in Smooth Water for a Prismatic Float Having an Angle of Dead Rise of  $30^{\circ}$ . NACA TN 1325, 1947.
4. Edge, Philip M., Jr.: Hydrodynamic Impact Loads in Smooth Water for a Prismatic Float Having an Angle of Dead Rise of  $40^{\circ}$ . NACA TN 1775, 1949.
5. Batterson, Sidney A.: The NACA Impact Basin and Water Landing Tests of a Float Model at Various Velocities and Weights. NACA Rep. 795, 1944. (Supersedes NACA WR L-163.)
6. Wagner, Herbert: Über Stoss- und Gleitvorgänge an der Oberfläche von Flüssigkeiten. Z.a.M.M., Bd. 12, Heft 4, Aug. 1932, pp. 193-215.
7. Pabst, Wilhelm: Landing Impact of Seaplanes. NACA TM 624, 1931.

TABLE I

IMPACT-LOADS DATA FROM TESTS OF PRISMATIC FLOAT WITH AN ANGLE OF DEAD RISE OF  $10^\circ$ 

Run	At contact		At $(n_1)_{\max}$				At $z_{\max}$			At rebound	
	$\dot{z}_0$ , fps	$\dot{x}_0$ , fps	t, sec	$n_1$ , g units	z, ft	$\dot{z}$ , fps	t, sec	$n_1$ , g units	z, ft	t, sec	$\dot{z}$ , fps
$\tau = 3^\circ$											
1	10.5	41.0	0.027	7.2	0.26	8.5	0.180	0.3	0.51	0.630	-1.0
2	10.4	40.6	.024	7.1	.25	8.5	.184	.4	.50	.659	-.7
3	10.2	25.6	.024	6.4	.27	8.7	.204	.5	.67	No exit	No exit
4	10.5	25.7	.030	6.2	.27	8.6	.208	.3	.67	No exit	No exit
5	10.9	57.3	.026	8.6	.27	8.6	.110	.7	.44	.294	-1.7
6	3.6	93.5	.058	2.2	.17	1.9	.084	1.6	.20	.210	-2.1
7	4.5	93.5	.056	2.9	.20	2.5	.087	2.0	.21	.194	-2.3
8	7.1	91.7	.037	5.5	.24	5.1	.070	2.6	.29	.197	-2.8
9	6.7	90.9	.041	5.0	.25	4.5	.080	2.1	.28	.195	-2.6
10	4.2	91.7	.054	3.0	.20	2.5	.075	2.3	.23	.193	-2.4
11	3.4	90.9	.056	2.1	.16	1.9	.090	1.6	.19	.200	-2.0
12	10.6	54.7	.029	7.7	.27	8.1	.110	.6	.44	.406	-1.5
13	10.7	38.8	.029	7.4	.25	9.5	.190	.3	.54	.693	-1.0
14	10.8	25.3	.028	6.5	.30	9.6	.205	.4	.72	No exit	No exit
$\tau = 12^\circ$											
15	2.9	96.2	0.061	2.6	0.16	1.2	0.070	2.6	0.16	0.139	-2.9
16	4.4	90.9	.058	4.4	.20	1.5	.069	4.1	.20	.132	-5.2
17	6.3	91.3	.049	6.2	.24	3.1	.061	5.5	.26	.126	-3.6
$\tau = 20^\circ$											
18	2.5	89.3	0.078	2.1	0.12	0.3	0.080	2.0	0.12	0.140	-2.9
19	5.1	90.1	.053	5.5	.22	1.9	.065	5.0	.22	.128	-6.1
20	6.5	79.4	.053	5.9	.26	3.0	.065	5.4	.27	.132	-7.6
$\tau = 30^\circ$											
21	2.3	95.2	0.080	1.9	0.13	0.1	0.080	1.9	0.13	0.133	-2.5
22	4.5	89.3	.062	5.1	.18	.4	.062	5.0	.18	.120	-6.4
23	1.0	94.3	.090	.8	.06	.1	.090	.5	.06	.156	-1.1
24	5.7	78.4	.056	5.8	.25	1.9	.061	5.8	.25	.127	-8.5

OFFSETS OF MODEL

Station	Half-breadth	Height above datum line	
		Keel	China
0	0	15.71	15.71
14	10.0	3.86	14.37
29	16.0	1.48	9.00
38	17.8	.73	6.83
47	19.0	.20	4.84
58	19.9	0	3.45
87.25	20.5	0	3.86
120.75	20.5	0	3.86

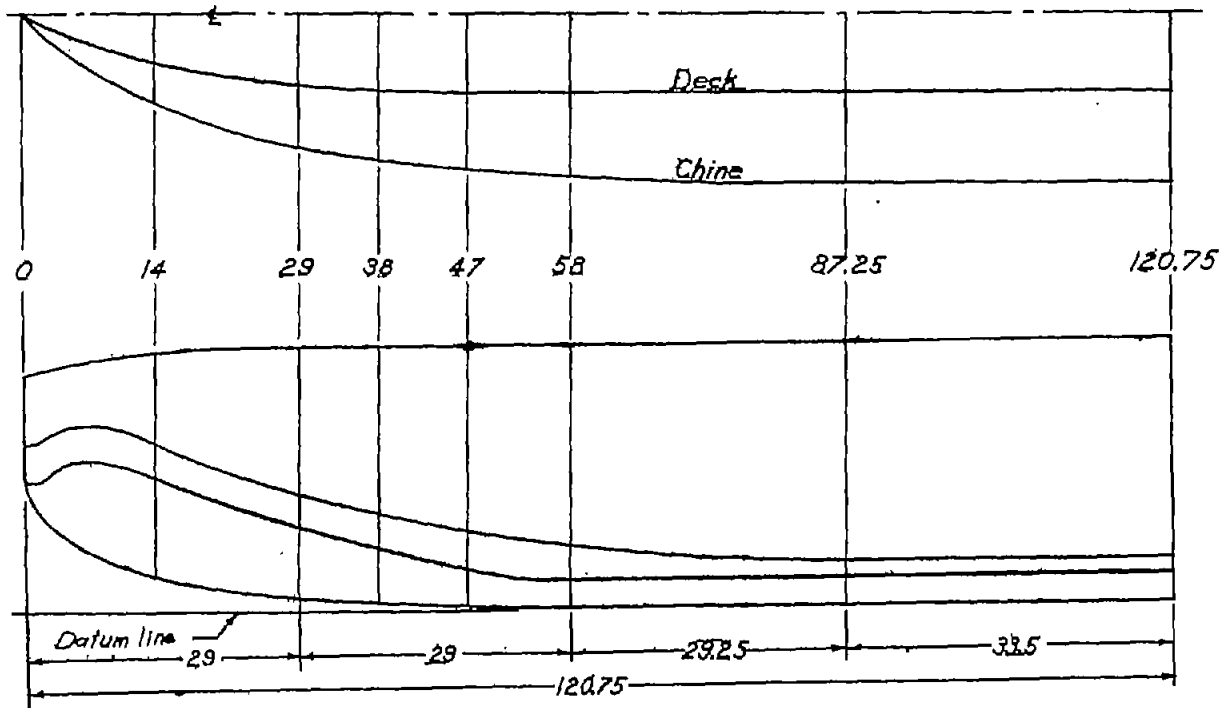
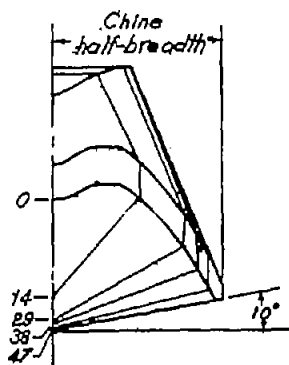


Figure 1.- Lines of prismatic float with an angle of dead rise of 10°. (All dimensions are in inches.)

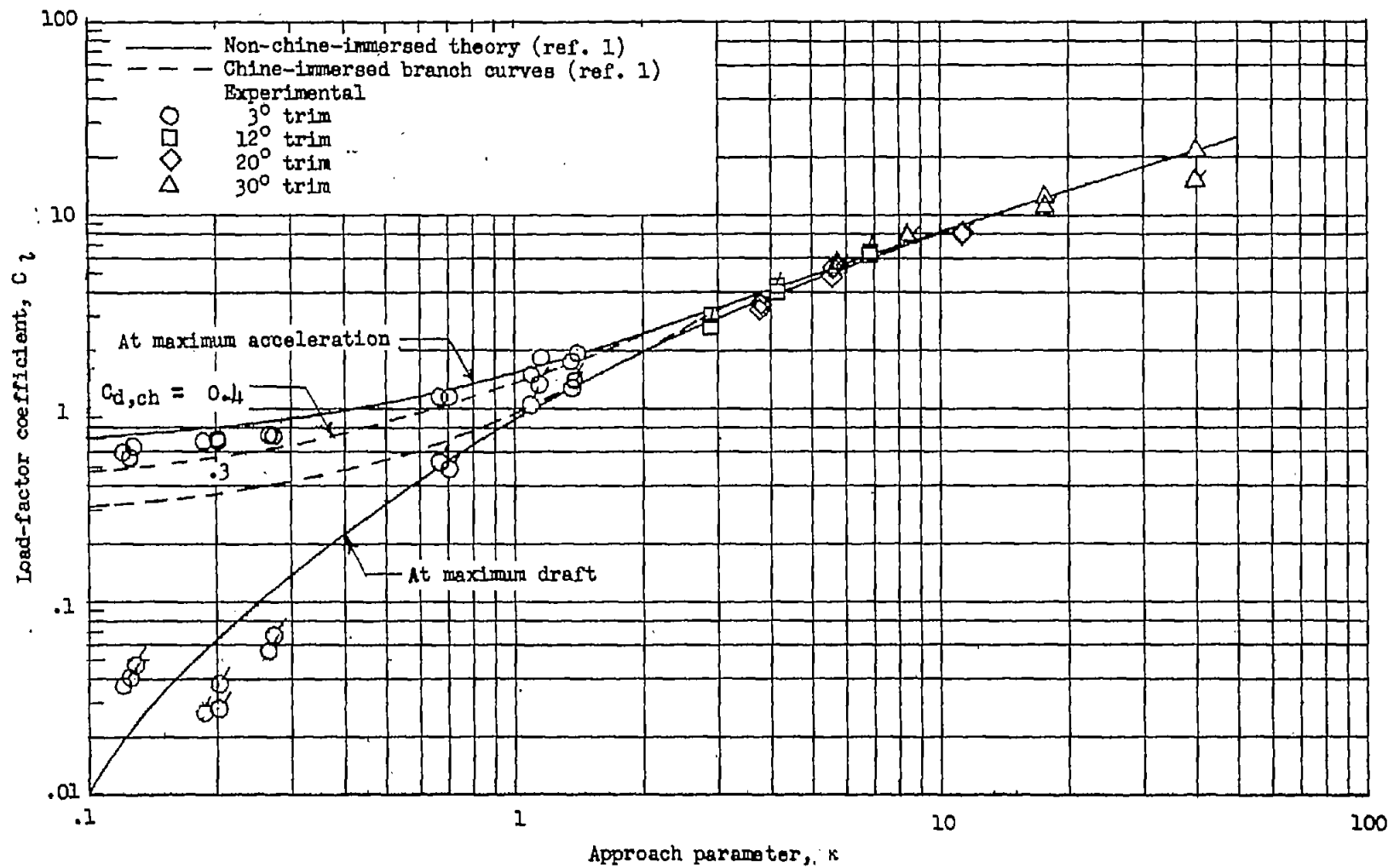


Figure 2.- Variation of load-factor coefficient with approach parameter.  
 Flagged symbols indicate points at maximum draft.

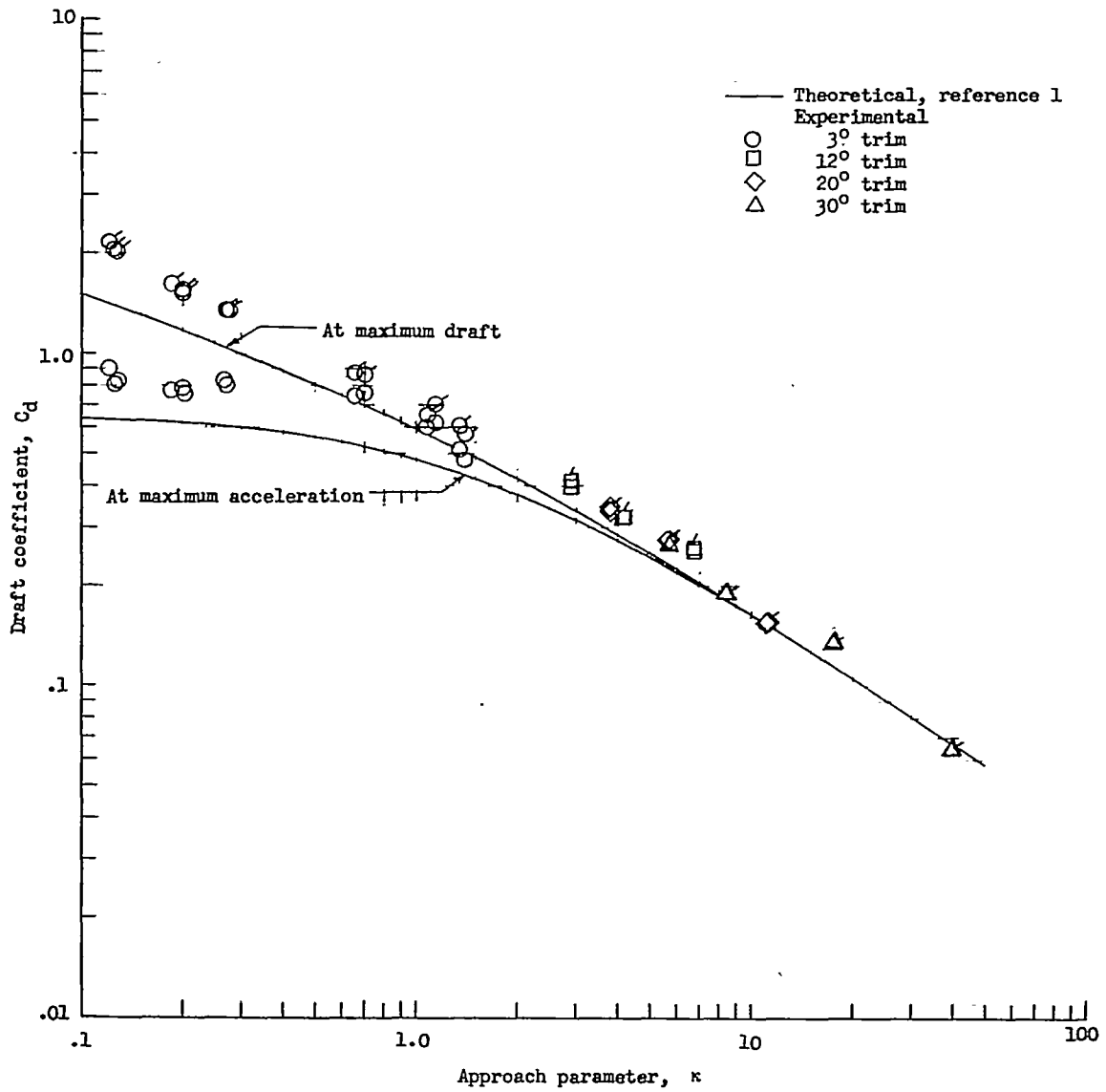


Figure 3.- Variation of draft coefficient with approach parameter. Flagged symbols indicate points at maximum draft.



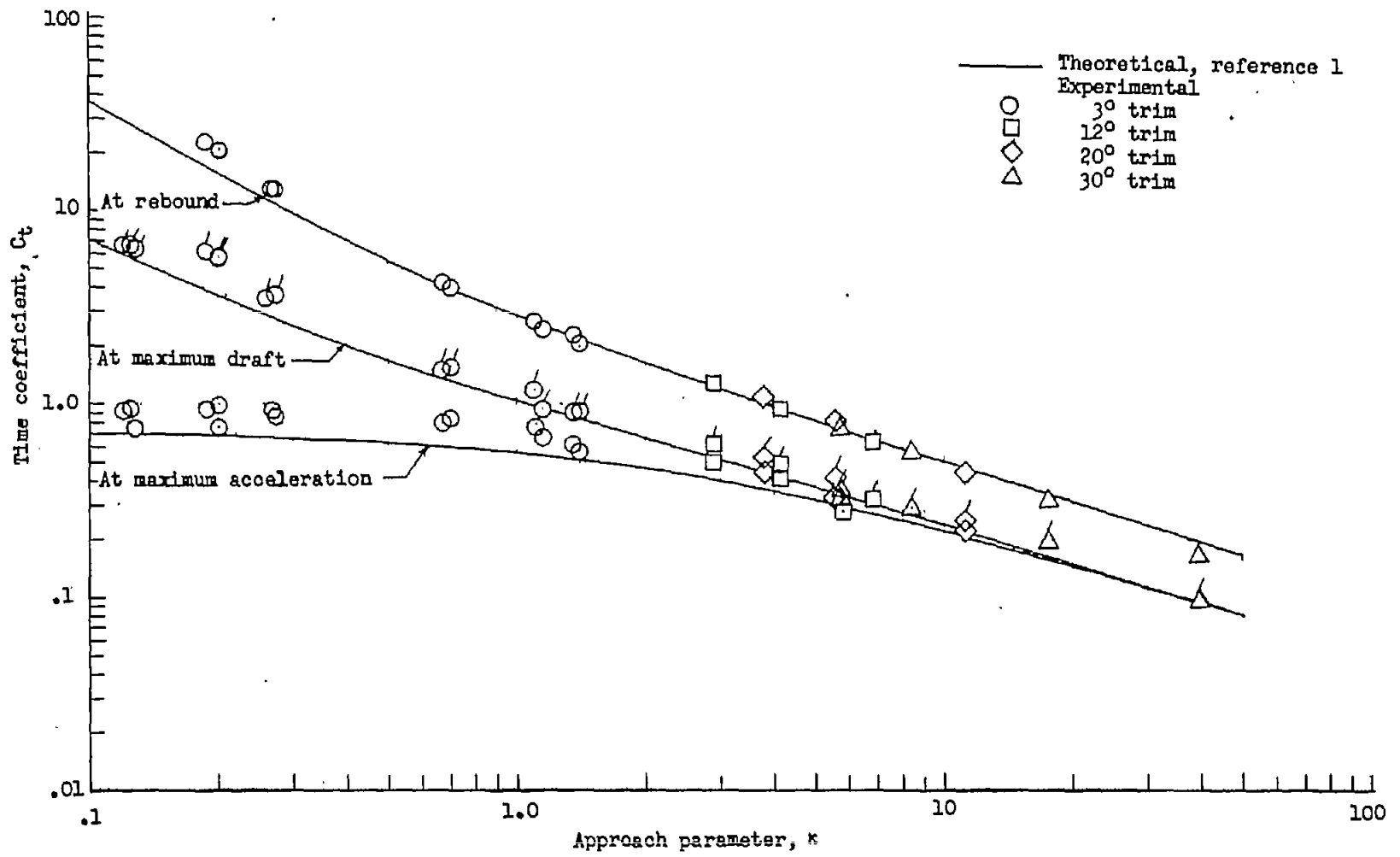


Figure 4.- Variation of time coefficient with approach parameter.  
Flagged symbols indicate points at maximum draft.

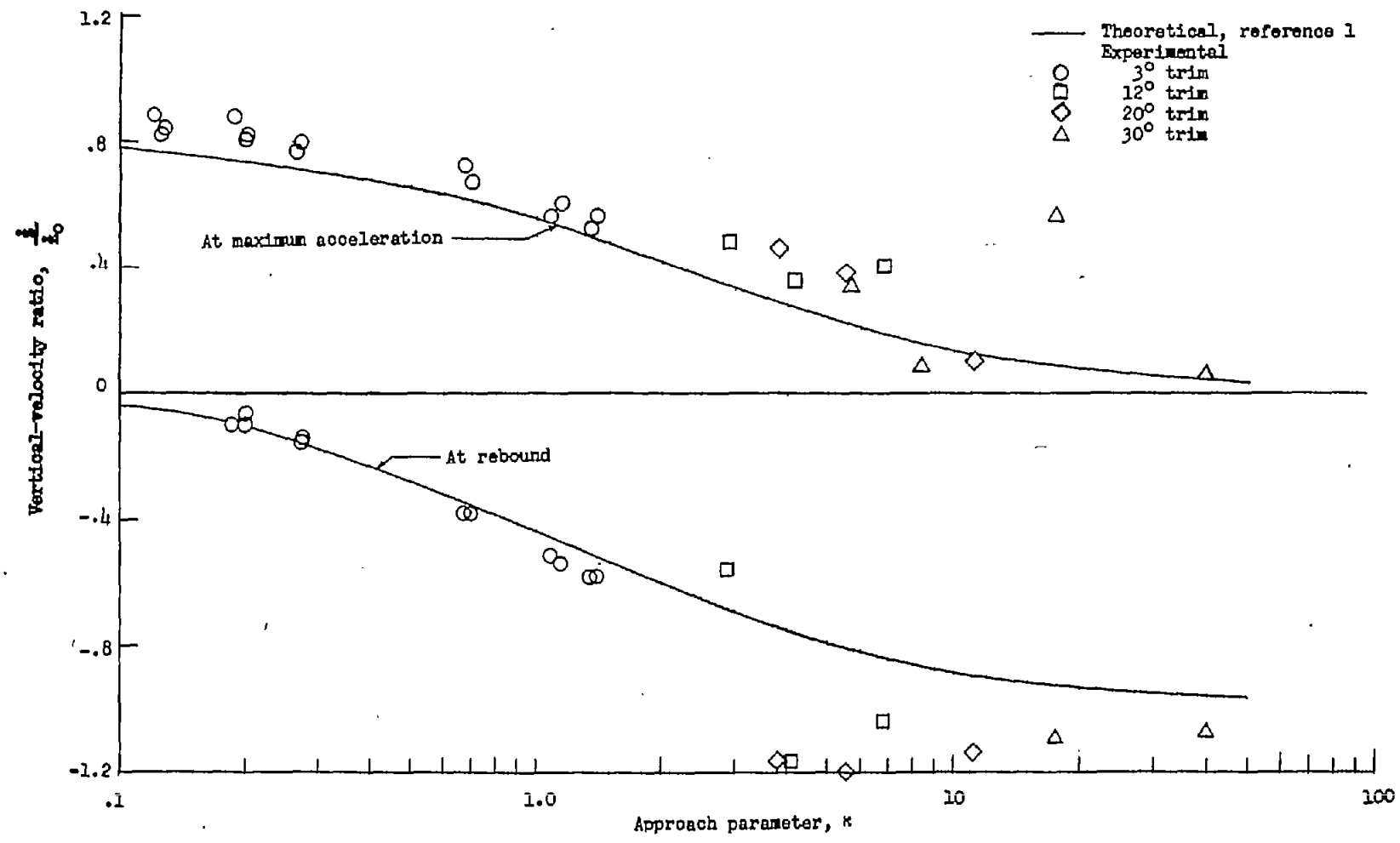


Figure 5.- Variation of vertical velocity with approach parameter.

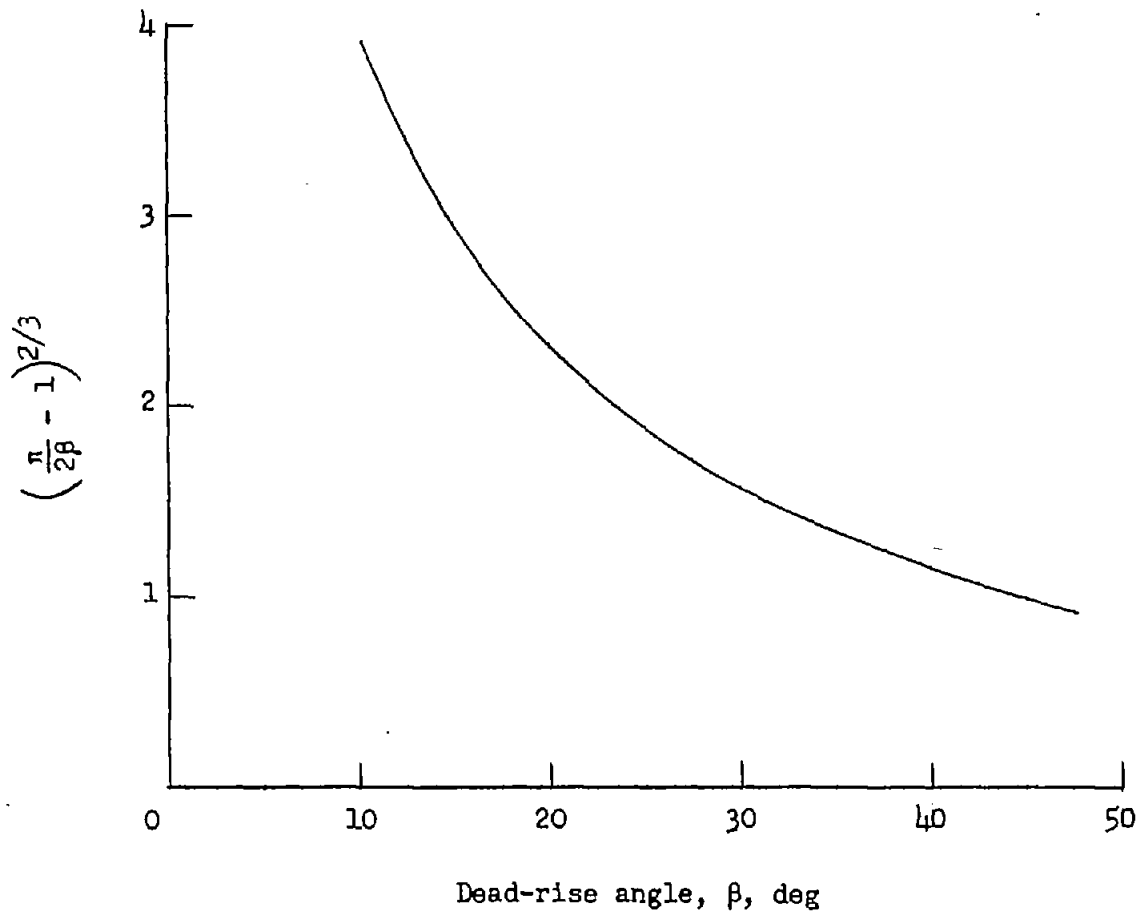


Figure 6.- Variation of  $\left(\frac{\pi}{2\beta} - 1\right)^{2/3}$  with dead-rise angle.

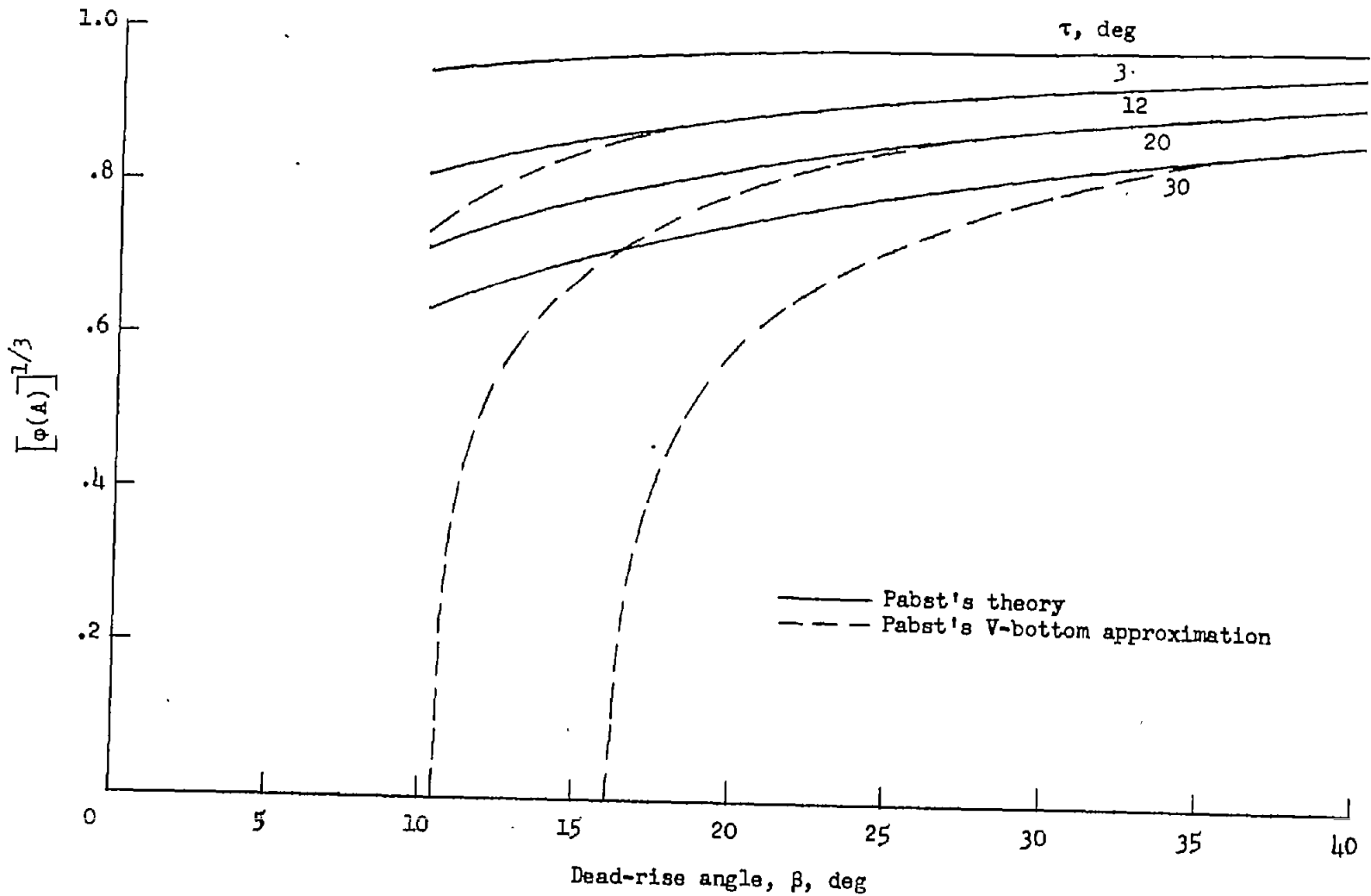


Figure 7.- Variation of Pabst's aspect-ratio factor with angle of dead rise.

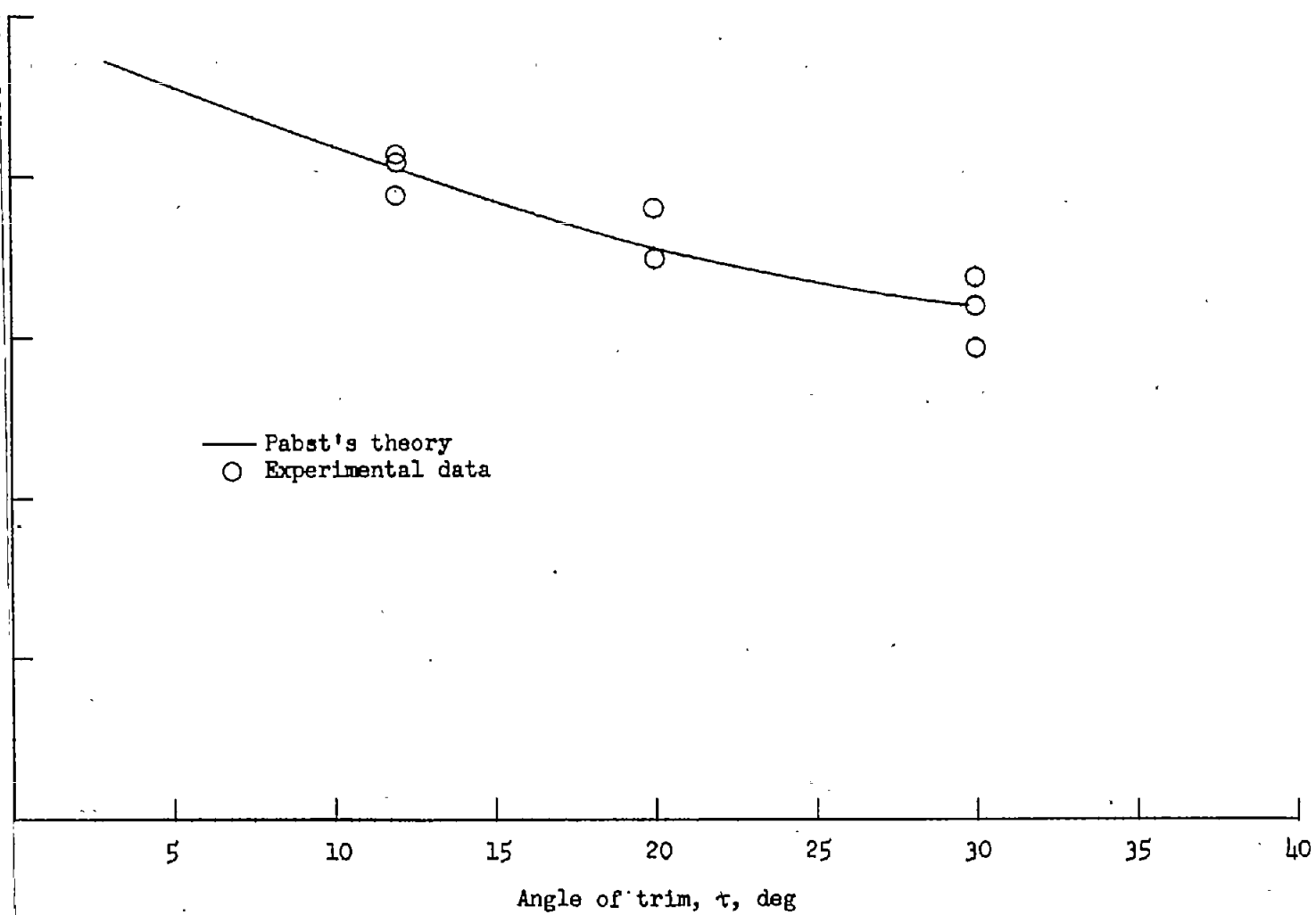


Figure 8.- Variation of aspect-ratio factor with angle of trim for float with an angle of dead rise of  $10^\circ$ .